

## Phase diagrams of period-4 spin chains consisting of three kinds of spins

Ken'ichi Takano

Laboratory of Theoretical Condensed Matter Physics and Research Center for Advanced Photon Technology,  
Toyota Technological Institute, Nagoya 468-8511, Japan

(Received March 22, 2024)

We study a period-4 antiferromagnetic mixed quantum spin chain consisting of three kinds of spins. When the ground state is singlet, the spin magnitudes in a unit cell are arrayed as  $(s-t; s; s+t; t; s)$  with integer or half-odd integer  $s$  and  $t$  ( $0 < t < s$ ). The spin Hamiltonian is mapped onto a nonlinear model (NLSM) in a previously developed method. The resultant NLSM includes only two independent parameters originating from four exchange constants for fixed  $s$  and  $t$ . The topological angle in the NLSM determines the gapless phase boundaries between disordered phases in the parameter space. The phase diagrams for various  $s$  and  $t$  show rich structures. We systematically explain the phases in the singlet-cluster-solid picture.

PACS numbers: 75.10.Jm, 75.30.Kz

## I. INTRODUCTION

The lowest spin excitation for a homogeneous antiferromagnetic spin chain has a gap if the spin magnitude is an integer, and has no gap if it is a half-odd integer. Haldane conjectured this proposition by mapping the spin chain onto the nonlinear model (NLSM) [1]. From the topological term of the NLSM, we know whether the spin excitation is gapless or not. Mapping to the NLSM is now recognized as one of powerful methods to examine quantum spin systems. Various aspects of the NLSM method are found in Refs. [2,3,4].

Analyses using the NLSM have been extended to inhomogeneous spin chains. The first step has been done by Aleck [5,6]. He reformulated the NLSM method in an operator formalism in which spin operators are transformed in pairs. Due to the pair transformation, his formalism is applicable to a spin chain with bond alternation. Then the exchange constant is inhomogeneous with period 2 but the spin magnitude is still homogeneous. Results by the NLSM method qualitatively agree with numerical and experimental results [7,8,9].

The NLSM method for a general inhomogeneous spin chain with arbitrary period is given, if the ground state is singlet, in a previous paper [10]. The inhomogeneity is not only for the exchange constant but also for the spin magnitude. The derivation of the NLSM is based on dividing the spin chain into blocks and simultaneously transforming the spin variables belonging to a block in a path integral formalism. From the topological term, the gapless condition for the spin excitation is obtained as an equation, which we have called the gapless equation. The gapless equation determines the phase boundaries in the ground-state phase diagram. This method is quite general, and is applicable to various spin chains.

A period-4 chain is the simplest nontrivial case in which more than one kind of spins can be mixed under condition that the ground state is singlet. We have applied the NLSM method to a period-4 chain consisting of two kinds of spins and presented the phase diagram in the parameter space of exchange constants [11,12]. When

the magnitudes of two kinds of spins are  $s_a$  and  $s_b$ , only the array of  $(s_a, s_a, s_b, s_b)$  in a unit cell consists with a singlet ground state. We have constructed an NLSM and then the gapless equation for this case following the general procedure [10]; Fukui and Kawakami also derived the NLSM in a different standpoint [13]. We constructed phase diagrams from the NLSM and found that they generally consist of many disordered phases. To understand various phases we have proposed the singlet-cluster-solid (SCS) picture, which is an extension of the valence-bond-solid (VBS) picture [14]. The SCS picture systematically explains all phases for any values of  $s_a$  and  $s_b$ . A simple version of the SCS picture is seen in the case of  $s_a = s_b = \frac{1}{2}$  [15]. In the case of  $s_a = \frac{1}{2}$  and  $s_b = 1$ , numerical calculation has been performed [16]. The phase diagram by the NLSM method qualitatively agrees with the numerical phase diagram.

In this paper, we study a period-4 spin chain consisting of three kinds of spins. Systematic treatment of this problem seems to be difficult due to many possibilities in the choice of the spin kinds. However, the condition that the ground state is singlet fairly restricts allowed combinations. In fact, the spin magnitudes in a unit cell must be generally arrayed as  $(s-t; s; s+t; t; s)$  with integer or half-odd integer  $s$  and  $t$  ( $0 < t < s$ ), as will be seen. The spin chain has a modulation in the spin magnitude around average  $s$ ; hence it is interesting to compare results for different  $t$  and the same  $s$ . The exchange constants are also periodic with period 4 and then there are three parameters except for an energy unit. The spin Hamiltonian is mapped onto an NLSM in the general method [10]. The resultant NLSM shows that the number of relevant parameters is not three but two. The phase diagrams for various  $s$  and  $t$  determined by the gapless equation show rich phase structures [17]. We systematically explain the phases in the SCS picture.

This paper is organized as follows. In Sec. II, we introduce the Hamiltonian for the period-4 spin chain consisting of three kinds of spins with a singlet ground state, and parameterize the exchange constants. In Sec. III, the spin Hamiltonian is transformed to an NLSM. From the

topological term of the NLSM, the gapless equation to determine phase boundaries is derived. In Sec. IV, phase diagrams are drawn by the gapless equation for various spin magnitudes. Features of the phases are mentioned. In Sec. V, the ground states of the phases are explained by the SCS picture. Section VI is devoted to summary and discussion.

## II. HAMILTONIAN

The spin Hamiltonian with period 4 is generally written as

$$H = \sum_{j=1}^{N/4} (J_1 S_{4j+1} S_{j+2} + J_2 S_{4j+2} S_{j+3} + J_3 S_{4j+3} S_{j+4} + J_4 S_{4j+4} S_{j+5}); \quad (1)$$

where  $S_j$  is the spin at site  $j$  with magnitude  $s_j$ . The number of lattice sites is  $N$ , the lattice spacing is  $a$  and the system size is  $L = aN$ . We only consider the antiferromagnetic exchange interaction ( $J_i > 0$ ).

Since the system is periodic with period 4 in the spin magnitude as well as in the exchange constant, we generally have 4 different spin magnitudes ( $s_1, s_2, s_3, s_4$ ) in a unit cell. A unit cell is illustrated in Fig. 1. The values of the spin magnitudes are restricted in order that the system has a singlet ground state. Following the Lieb-Mattis theorem [18], a singlet ground state is realized if the system satisfies the restriction

$$s_1 - s_2 + s_3 - s_4 = 0; \quad (2)$$

otherwise the system has a ferrimagnetic ground state. We have treated the case that three kinds of spins are mixed. To consist with the restriction (2), the spin magnitudes must be of the following form :

$$(s_1; s_2; s_3; s_4) = (s - t; s; s + t; s); \quad (3)$$

where  $s$  and  $t$  are positive integers or half-odd integers satisfying  $s > t \geq 0$ . The spin configuration (3) is regarded as a modulation against the uniform configuration  $(s; s; s; s)$ .

We parameterize the exchange constants as

$$\begin{aligned} J_1 &= \frac{J}{1 + \epsilon}; & J_2 &= \frac{J^0}{1}; \\ J_3 &= \frac{J^0}{1 + \epsilon}; & J_4 &= \frac{J}{1}; \end{aligned} \quad (4)$$

where  $\epsilon$  is the distortion parameter describing the asymmetry between exchange constants  $J_4$  and  $J_1$  ( $J_2$  and  $J_3$ ) on the both sides of a spin with  $s_1$  ( $s_3$ ).

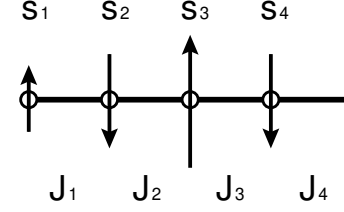


FIG. 1. Spin magnitudes and exchange constants of the Hamiltonian (1) with Eqs. (3) and (4) in a unit cell.

## III. MAPPING TO THE NONLINEAR MODEL

The expectation value of a spin operator in a coherent state is expressed as

$$\langle S_j \rangle = (1)^j s_j n_j \quad (5)$$

with a unit vector  $n_j$ . The partition function  $Z$  at temperature  $1 = \beta$  is then represented as

$$Z = \int \prod_j d[n_j] \prod_j (n_j^2 - 1) e^{-\beta S}; \quad (6)$$

$$\begin{aligned} S &= i \sum_{j=1}^{N/4} (1)^j s_j w[n_j] \\ &+ \frac{1}{2} \sum_{j=1}^{N/4} \sum_{l=1}^{N/4} J_{jl} s_j s_{j+l} (n_j - n_{j+l})^2; \end{aligned} \quad (7)$$

In the action (7), the first term comes from the Berry phase and  $w[n_j]$  is the solid angle which the unit vector  $n_j$  forms in the period  $2\pi$ .

We have derived the NLSM action starting from the action (7) for the general periodic case [10]. The derivation is based on dividing the spin chain into blocks and transforming the spin variables in a block into new ones. In the present case, by choosing unit cells as blocks, the transformation for the  $p$ th block is written as

$$\begin{aligned} n_{4p+1} &= \frac{3}{4} m(p) + \frac{1}{4} m(p-1) + aL_1(p); \\ n_{4p+2} &= m(p) + aL_2(p); \\ n_{4p+3} &= \frac{3}{4} m(p) + \frac{1}{4} m(p+1) + aL_3(p); \\ n_{4p+4} &= \frac{1}{2} m(p) + \frac{1}{2} m(p+1) + aL_4(p); \end{aligned} \quad (8)$$

where  $f_m(p)$  are gradually changing unit vectors and  $f_{L_q}(p)$  are small fluctuations. This transformation does not change the number of the original degrees of freedom [10]. Integrating out the fluctuations  $f_{L_q}(p)$  and taking the continuum limit, we obtain the effective action [19]:

$$S_e = \int_0^Z d \int_0^Z dx \frac{1}{J^{(1)}} m^2 (\partial_m \partial_{x,m}) + \frac{1}{2aJ^{(1)}} \frac{J^{(1)}}{J^{(2)}} \frac{J^{(0)}}{J^{(1)}} (\partial_m)^2 + \frac{a}{2} J^{(0)} (\partial_{x,m})^2 ; \quad (9)$$

where

$$\frac{1}{J^{(0)}} = \frac{1}{2s} \frac{1}{J(s+t)} + \frac{1}{J^0(s+t)} ; \quad (10)$$

$$\frac{1}{J^{(1)}} = \frac{s}{4s} \frac{t}{J(s+t)} + \frac{1}{J^0(s+t)} + \frac{d}{J^0(s+t)} ; \quad (11)$$

$$\frac{1}{J^{(2)}} = \frac{1}{4s(s+t)} \frac{s^2}{J} \frac{t^2}{J^0} + \frac{s^2+t^2}{J^0} + \frac{s^2}{J^0} \frac{t^2}{J^0} d ; \quad (12)$$

We have used the effective distortion parameter

$$d = \frac{J^0}{J} ; \quad (13)$$

It is remarkable that two distortion parameters  $s$  and  $t$  appear only in a single parameter  $d$ . Hence the system is characterized by only a pair of parameters,  $(J^0=J; d)$ . The value of  $d$  is restricted as

$$|d| < 1 + \frac{J^0}{J} ; \quad (14)$$

because  $|d| < 1$  and  $|d| < 1$  from Eq. (4).

The action (9) is of the standard form of the NLSM :

$$S_{st} = \int_0^Z d \int_0^Z dx \frac{1}{4} m^2 (\partial_m \partial_{x,m}) + \frac{1}{2gv} (\partial_m)^2 + \frac{v}{2g} (\partial_{x,m})^2 \quad (15)$$

with the topological angle  $\theta$ , the coupling constant  $g$  and the spin wave velocity  $v$ . Comparing Eq. (9) to Eq. (15), is given as

$$v = 4 \frac{J^{(0)}}{J^{(1)}} ; \quad (16)$$

#### IV . P H A S E D I A G R A M S

The NLSM has a gapless excitation when  $s+t$  is a half-odd integer. From Eq. (16), this condition is rewritten as the gapless equation:

$$\frac{1}{J^{(1)}} = \frac{2l_0}{4} \frac{1}{J^{(0)}} ; \quad (17)$$

where  $l_0$  is an integer. For each  $l_0$ , this equation determines a boundary between disordered phases if it has a solution.

Substituting Eqs. (10) and (11) into Eq. (17), we have

$$d = \frac{1}{2} \frac{s}{s+t} + \frac{1}{s+t} \frac{1}{J^{(0)}} \frac{J^0}{J} \quad (18)$$

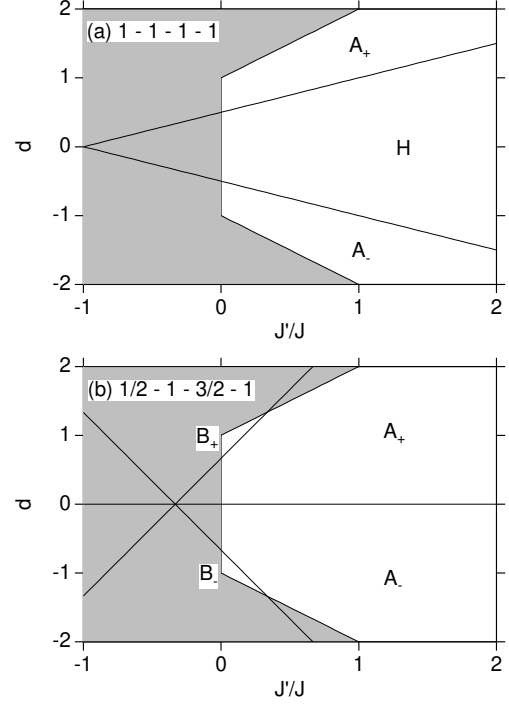


FIG. 2. The phase diagrams of  $s=1$  for (a)  $t=0$ , and (b)  $t=1/2$ . Unshaded regions are physical.

with  $l = l_0 + 2t + 1$ . A phase boundary is a straight line in the parameter space of  $(J^0=J; d)$ . Allowed values of integer  $l$  satisfying Eq. (14) are

$$l = 1; 2; \dots; 2(s+t) ; \quad (19)$$

Thus we have found that there are  $2(s+t) + 1$  phases separated by  $2(s+t)$  gapless phase boundaries. All of them go through the point

$$\left( \frac{s}{s+t}; 0 \right) ; \quad (20)$$

In the special case of  $d=0$ , Eq. (18) reduces to  $l = s+t + \frac{1}{2}$ . Then, the system has a spin gap when  $s_3 (= s+t)$  is an integer, while it has no spin gap when  $s_3$  is a half-odd integer. This is an extended version of Haldane's proposition for  $t=0$  and  $J^0=J$  to cases with period-4 modulation with respect to the spin magnitude and the exchange interaction. The condition  $d=0$  (i.e.  $J + J^0 = 0$ ) is satisfied even for nonzero  $s$  and  $t$ . This means that effects of distortions can be canceled.

In Fig. 2, we present phase diagrams for  $s=1$ . Figure 2(a) is for  $s=1$  and  $t=0$ ; spins are arrayed as 1-1-1-1 in a unit cell. Then the spin magnitude is homogeneous, while the exchange interaction is modulated with period 4. The shaded regions are not physical because of Eq. (14) and  $J^0=J > 0$ . There are three phases labeled by  $A_+$ ,  $H$ , and  $A_-$ . Phase  $H$  is the Haldane phase since it includes the point  $(1, 0)$  which represents the uniform  $s=1$  spin

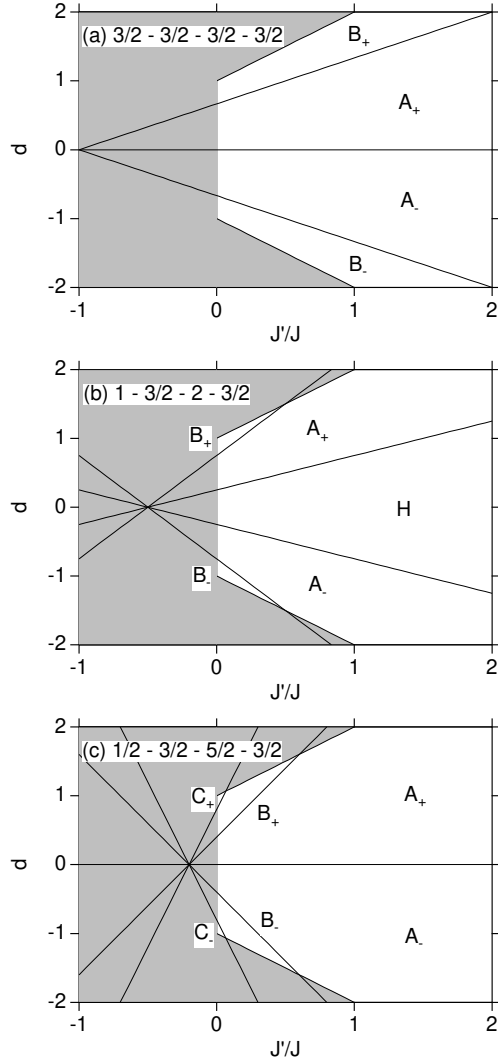


FIG. 3. The phase diagrams of  $s = \frac{3}{2}$  for (a)  $t = 0$ , (b)  $\frac{1}{2}$ , and (c) 1. Unshaded regions are physical.

chain. Two phases  $A_+$  and  $A_-$  appear, when the effective distortion is strong. Figure 2(b) is for  $s = 1$  and  $t = \frac{1}{2}$ ; spins are arrayed as  $\frac{1}{2}-1-\frac{3}{2}-1$  in a unit cell. There are four phases labeled by  $B_+$ ,  $A_+$ ,  $A_-$ , and  $B_-$ . In contrast to the case of (a), the system is on a boundary when there is no effective distortion ( $d = 0$ ). It is noticed that the phases  $B_+$  and  $B_-$  appear, when  $J^0 = J < 1$ . All the phases in Figs. 2(a) and (b) are interpreted by means of the SCS picture in the next section.

In Fig. 3, we present phase diagrams for  $s = \frac{3}{2}$ . Figure 3(a) is for  $s = \frac{3}{2}$  and  $t = 0$ ; spins are arrayed as  $\frac{3}{2}-\frac{3}{2}-\frac{3}{2}-\frac{3}{2}$  in a unit cell. Only the exchange interaction is modulated with period 4. There are 4 phases labeled by  $B_+$ ,  $A_+$ ,  $A_-$ , and  $B_-$ . These phases, including  $B_+$  and  $B_-$  for strong distortion, develop from small  $J^0 = J$  to large  $J^0 = J$ . Figure 3(b) is for  $s = \frac{3}{2}$  and  $t = \frac{1}{2}$ ; spins are arrayed as  $1-\frac{3}{2}-2-\frac{3}{2}$  in a unit cell. There are 5 phases labeled by  $B_+$ ,

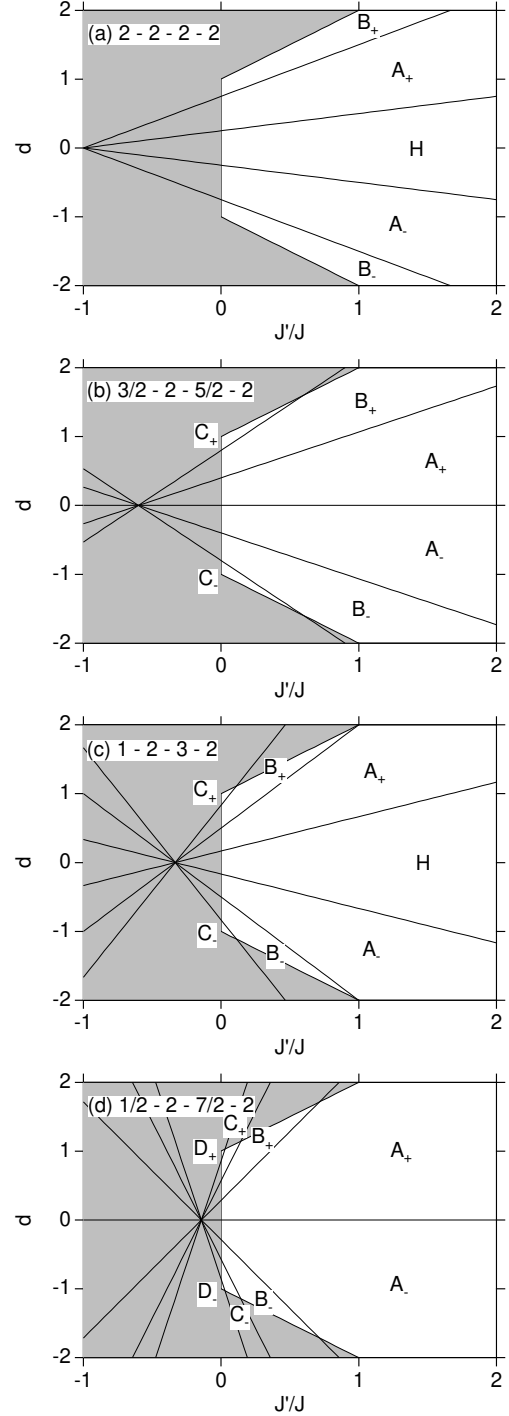


FIG. 4. The phase diagrams of  $s = 2$  for (a)  $t = 0$ , (b)  $\frac{1}{2}$ , (c) 1, and (d)  $\frac{3}{2}$ . Unshaded regions are physical.

$A_+$ ,  $H$ ,  $A_-$ , and  $B_-$ . Phases  $B_+$  and  $B_-$  appear only when  $J^0=J < 1$ . Figure 3(c) is for  $s=\frac{3}{2}$  and  $t=1$ ; spins are arrayed as  $\frac{1}{2}-\frac{3}{2}-\frac{5}{2}-\frac{3}{2}$  in a unit cell. There are 6 phases labeled by  $C_+$ ,  $B_+$ ,  $A_+$ ,  $A_-$ ,  $B_-$ , and  $C_-$ . Phases  $C_+$ ,  $B_+$ ,  $B_-$ , and  $C_-$  appear only when  $J^0=J < 1$ ;  $C_+$  and  $C_-$  are for strong distortion and for very small  $J^0=J$ . In the case of (a), the system is on a gapless boundary when there is no effective distortion ( $d=0$ ). All the phases in Figs. 3(a), (b) and (c) are interpreted by means of the SCS picture in the next section.

In Fig. 4, we present phase diagrams for  $s=2$ . Figures 4(a), (b), (c) and (d) are for  $t=0$ ,  $t=\frac{1}{2}$ ,  $t=1$ , and  $t=\frac{3}{2}$ , respectively; spins are arrayed as 2-2-2-2,  $\frac{3}{2}-2-\frac{5}{2}-2$ , 1-2-3-2, and  $\frac{1}{2}-2-\frac{7}{2}-2$  in a unit cell. Phase  $H$  for small  $d$  in Figs. 4(a) and (c) is the  $s=2$  Haldane phase, which includes the point  $(1, 0)$ . In the cases of (b) and (d), the system is on a gapless boundary when there is no effective distortion ( $d=0$ ). Some phases develop from small  $J^0=J$  to large  $J^0=J$ , and the others are restricted in the region  $J^0=J < 1$ .

#### V. SINGLET-CLUSTER-SOLID PICTURE

Disordered phases in the phase diagrams are explained in the SCS picture, which includes the VBS picture as a special case. In the SCS picture, a spin with more than  $\frac{1}{2}$  magnitude is decomposed into  $\frac{1}{2}$  spins. The original spin state is retrieved by symmetrizing the states of the decomposed  $\frac{1}{2}$  spins at each site. A disordered state is represented by a regular array of local singlet clusters of even numbers of  $\frac{1}{2}$  spins, while a state in the VBS picture is a direct product of only singlet dimers.

The SCS pictures for the phase diagrams of  $s=1$  in Fig. 2 are shown in Figs. 5 and 6. Figure 5 explains the phase diagram in Fig. 2(a) for the 1-1-1-1 spin chain ( $s=1$ ,  $t=0$ ). For each picture, a small circle represents a  $\frac{1}{2}$  spin; an original  $s=1$  spin is decomposed into two  $\frac{1}{2}$  spins. A loop represents a singlet dimer of two  $\frac{1}{2}$  spins in it. A dashed line represents a spatially extended singlet state. Picture (a) ((e)) is for a state in the dimer phase  $A_+$  ( $A_-$ ), and has advantage for the exchange energy on  $J_2$  and/or  $J_4$  ( $J_1$  and/or  $J_3$ ) interactions because of positive (negative)  $d$ . Picture (c) is for a translationally invariant state in the Haldane phase  $H$ . These pictures are nothing but the VBS picture; a ground state is represented only by singlet dimers. Pictures (b) and (d) are for states between  $A_+$  and  $H$ , and between  $H$  and  $A_-$ , respectively; each picture includes an extended singlet state (dashed line) contributing to a gapless excitation.

Figure 6 explains the phase diagram in Fig. 2(b) for the  $\frac{1}{2}-1-\frac{3}{2}-1$  spin chain ( $s=1$ ,  $t=\frac{1}{2}$ ). Pictures (c) and (e) are for dimer states  $A_+$  and  $A_-$ , respectively. The state (c) ((e)) has advantage for the exchange energy on  $J_2$  and/or  $J_4$  ( $J_1$  and/or  $J_3$ ) interactions because of positive (negative) distortion  $d$ . Pictures (a) and (g) are for singlet cluster states in the phases  $B_+$  and  $B_-$ , which

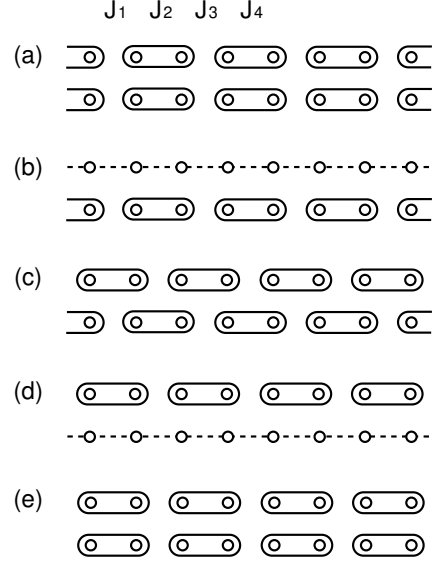


FIG. 5. The SCS pictures for the phases of  $s=1$  and  $t=0$ . They represent states for phases (a)  $A_+$ , (c)  $H$ , and (e)  $A_-$  in Fig. 2(a).  $H$  is the Haldane phase. They are the same as the VBS pictures in the present case. Gapless states on the phase boundaries are presented in (b), and (d).

are in the region of  $J^0=J < 1$ . In phase  $B_+$  ( $B_-$ ), a singlet cluster or dimer including a  $J_3$  ( $J_2$ ) interaction is the most unfavorable for the exchange energy because of large  $|J|$  and small  $J^0=J$ . Hence clusters of six  $\frac{1}{2}$  spins are formed to avoid singlet dimers at  $J_3$  ( $J_2$ ) interactions. Pictures (b), (d), and (f) are for gapless states on the phase boundaries, where extended states appear.

The SCS pictures for the phase diagrams of  $s=\frac{3}{2}$  in Fig. 3 are shown in Figs. 7, 8, and 9. Those for phase boundaries are not drawn to reduce the figure sizes. Figure 7 explains the phase diagram in Fig. 3(a) for the  $\frac{3}{2}-\frac{3}{2}-\frac{3}{2}-\frac{3}{2}$  spin chain ( $s=\frac{3}{2}$ ,  $t=0$ ). The SCS pictures represent the ground states in phases (a)  $B_+$ , (b)  $A_+$ , (c)  $A_-$ , and (d)  $B_-$ , and are the same as the VBS pictures. Picture (a) ((d)) is for the dimer phase  $B_+$  ( $B_-$ ), where the energy reduction on  $J_2$  and/or  $J_4$  ( $J_1$  and/or  $J_3$ ) interactions is the most favorable because of large  $|J|$ . Picture (b) ((c)) is for the phase  $A_+$  ( $A_-$ ), where the energy reduction on  $J_2$  and/or  $J_4$  ( $J_1$  and/or  $J_3$ ) interactions is favorable to some extent because of smaller but finite  $|J|$ .

Figure 8 explains the phase diagram in Fig. 3(b) for the  $1-\frac{3}{2}-2-\frac{3}{2}$  spin chain ( $s=\frac{3}{2}$ ,  $t=\frac{1}{2}$ ). The SCS pictures represent states in phases (a)  $B_+$ , (b)  $A_+$ , (c)  $H$ , (d)  $A_-$ , and (e)  $B_-$ . Picture (c) represents a Haldane-like state. With transitions (c) to (b) and (b) to (a), the number of dimers including  $J_3$  interactions decreases. This explains that  $d$  in  $B_+$  is larger than  $d$  in  $A_+$ , and  $d$  in  $A_+$  is larger than  $d$  in  $H$  as seen in Fig. 3(b). In particular, the SCS pictures in  $B_+$  and  $B_-$  include singlet clusters of six  $\frac{1}{2}$  spins. The large clusters are formed for  $J^0=J < 1$  to avoid

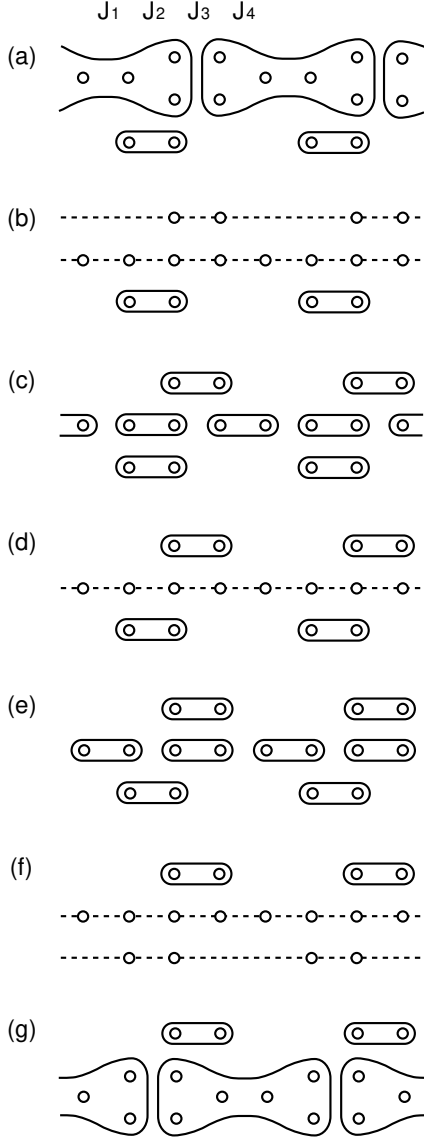


FIG. 6. The SCS pictures for the phases of  $s=1$  and  $t=\frac{1}{2}$ . They represent states for phases (a)  $B_+$ , (c)  $A_+$ , (e)  $A_-$ , and (g)  $B_-$  in Fig. 2(b). Gapless states on the phase boundaries are presented in (b), (d), and (f).

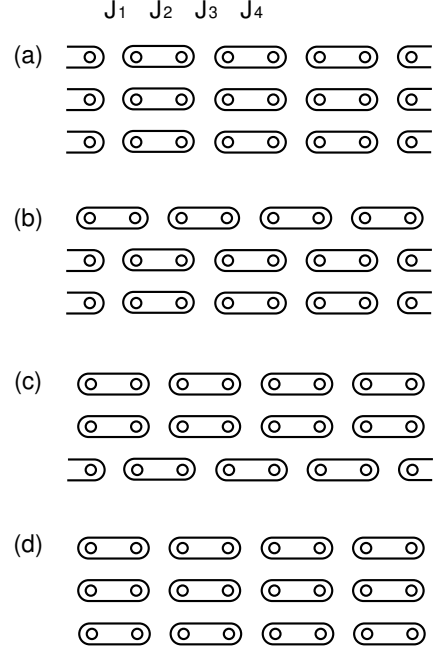


FIG. 7. The SCS pictures for the phases of  $s=\frac{3}{2}$  and  $t=0$ . They represent states for phases (a)  $B_+$ , (b)  $A_+$ , (c)  $A_-$ , and (d)  $B_-$  in Fig. 3(a). They are the same as the VBS pictures in the present case.

singlet dimers including  $J_3$  ( $J_2$ ) interactions.

Figure 9 explains the phase diagram in Fig. 3(a) for the  $\frac{1}{2}-\frac{3}{2}-\frac{5}{2}-\frac{3}{2}$  spin chain ( $s=\frac{3}{2}$ ,  $t=1$ ). The SCS pictures represent states in phases (a)  $C_+$ , (b)  $B_+$ , (c)  $A_+$ , (d)  $A_-$ , (e)  $B_-$ , and (f)  $C_-$ . Large singlet clusters of more than two  $\frac{1}{2}$  spins are formed in  $C_+$ ,  $B_+$ ,  $B_-$ , and  $C_-$  for  $J^0=J < 1$  again.

The SCS pictures of the ground states for arbitrary  $s$  and  $t$ , including the cases of  $s=2$  in Fig. 4, are similar to the above examples. Phases for small values of  $|t|$  are represented by VBS pictures, each of which consists of singlet dimers only. The number of possible VBS pictures is  $2(s-t)$ , and they are between the boundaries of  $|t|=2t$  and of  $|t|=2s+1$  in Eqs. (18) and (19). For larger  $d$  outside the VBS phases in the ( $J^0=J$ ,  $d$ ) space, there appear phases represented by SCS pictures which includes singlet clusters larger than dimers. Generally, as one moves from a phase to another accompanied by increasing (decreasing)  $d$  for  $d > 0$  ( $d < 0$ ), the number of singlet dimers on  $J_3$  ( $J_2$ ) interactions in the SCS picture decreases by one per unit cell. This explains the total number  $2(s+t)+1$  of the phases. The phases explained by SCS pictures including singlet clusters consisting of more than two  $\frac{1}{2}$  spins are restricted to small  $J^0=J$  regions. In fact, singlet dimers including  $J_3$  ( $J_2$ ) interactions are energetically unfavorable for small  $J^0=J$ , and the number of them can be reduced for  $t \neq 0$  if large clusters not including  $J_3$  ( $J_2$ ) interactions are formed.

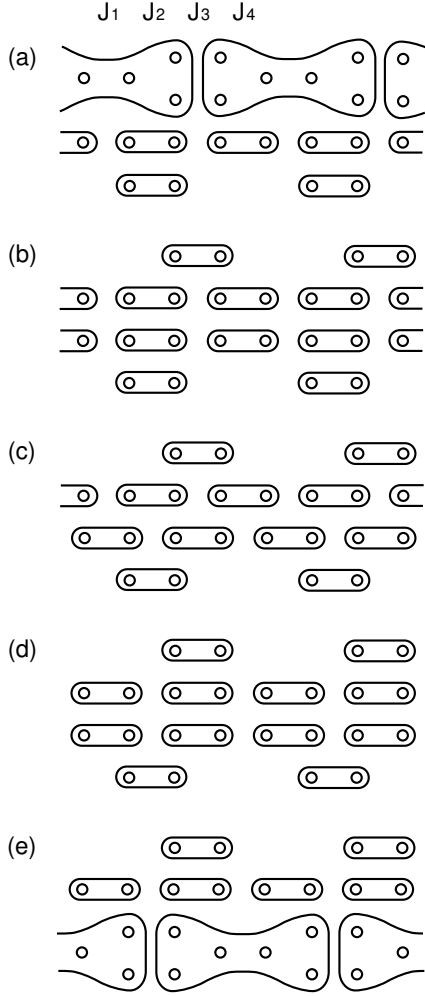


FIG. 8. The SCS pictures for the phases of  $s=\frac{3}{2}$  and  $t=\frac{1}{2}$ . They represent states for phases (a)  $B_+$ , (b)  $A_+$ , (c)  $H$ , (d)  $A_-$ , and (e)  $B_-$  in Fig. 3(b).

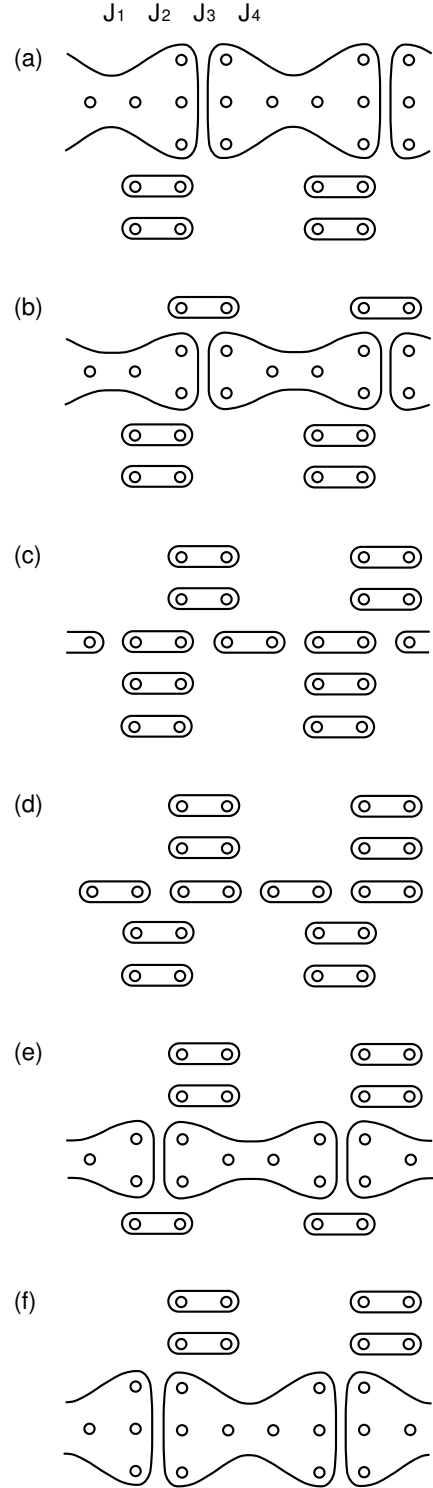


FIG. 9. The SCS pictures for the phases of  $s=\frac{3}{2}$  and  $t=1$ . They represent states for phases (a)  $C_+$ , (b)  $B_+$ , (c)  $A_+$ , (d)  $A_-$ , (e)  $B_-$ , and (f)  $C_-$  in Fig. 3(c).

We studied a period-4 antiferromagnetic mixed quantum spin chain consisting of three kinds of spins in the case that the ground state is singlet. The spin magnitudes in a unit cell must be arrayed as  $(s-t; s; s+t; s)$  with integer or half-odd integer  $s$  and  $t$  ( $0 \leq t < s$ ). The exchange constants in a unit cell are  $(J_1; J_2; J_3; J_4)$ ; i.e. there are three parameters except for an energy unit. The spin Hamiltonian is transformed to an NLSM by a previously developed method [10]. In the NLSM, we find that the number of relevant parameters is not three but two. One of them is a ratio  $J^0=J$  of the exchange energies without distortion, and the other is the effective distortion parameter  $d$ . By the gapless equation from the NLSM, we determined  $2s+2t$  phase boundaries between gapful/disordered phases in the  $(J^0=J, d)$  space for each pair of  $s$  and  $t$ . We explained systematically the disordered phases by means of the SCS pictures. In the case of  $d=0$ , the ground state is in a gapful Haldane-like phase for  $s+t$  being an integer, and is on a gapless phase boundary for  $s+t$  being a half-odd integer. When  $d$  increases (decreases) from  $d=0$ , singlet clusters including  $J_3$  ( $J_2$ ) interactions successively decreases with phase transitions. If  $t \neq 0$ , singlet clusters larger than dimers appear for large  $|t|$  and small  $J^0=J$ .

We discuss whether a change from an SCS state to another is a phase transition or not. For simplicity, we consider a part of a full SCS state as shown in Fig. 10. State (a) is a VBS state which is a direct product of singlet dimers. This state can gradually change to state (b) without a phase transition, because state (b) is formed by local modifications where a pair of dimers puts together into a singlet cluster of four spins. The change from (a) to (c) is similar. We have used picture (a) as a representative of (a), (b) and (c) in this paper. On the other hand, there is no way to locally modify dimers in (a) to form dimers in (d). That is, the change from (a) to (d) must be realized only by a global recombination of dimers or a phase transition. The wave function for (a) is symmetric but that for (d) is antisymmetric with respect to the spatial reflection about the vertical dotted line. An extended state in (e) appears under the transition where both the dimer states are collapsed.

Finally it is expected that materials realizing period-4 quantum spin chains will be synthesized and experimentally studied. The present paper (and Ref. [12]) will hopefully work as a guide to investigate such materials.

#### ACKNOWLEDGMENT

I thank Takashi Tonegawa and Kiyomio Kamoto for discussions on the  $\frac{1}{2}$ - $1$ - $\frac{3}{2}$ - $1$  spin chain. This work is supported by the Grant-in-Aid for Scientific Research from the Ministry of Education, Science, Sports and Culture, Japan.

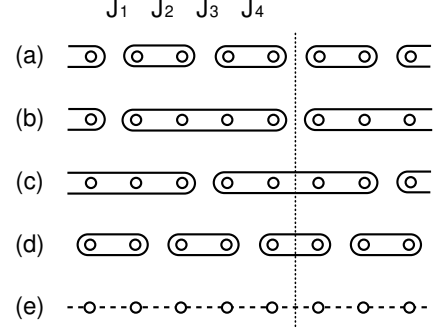


FIG. 10. A part of an SCS picture. Reflection with respect to the dotted vertical line is drawn to examine the necessity of a phase transition (see text).

- 
- [1] F.D.M. Haldane, Phys. Lett. 93A, 464 (1983); Phys. Rev. Lett. 50, 1153 (1983).
  - [2] I. A. A. "Field Theory Methods and Quantum Critical Phenomena" in Fields, Strings and Critical Phenomena, Les Houches 1988, eds. E. Brezin and J. Zinn-Justin, North-Holland, 1990.
  - [3] E. Fradkin, Field Theories of Condensed Matter Physics, Addison-Wesley Publishing, 1994.
  - [4] A.M. Tsvelick, Quantum Field Theories in Condensed Matter Physics, Cambridge University Press, 1995.
  - [5] I.A. A. Nucl. Phys. B 257, 397 (1985); 265, 409 (1986).
  - [6] I.A. A. and F.D.M. Haldane, Phys. Rev. B 36, 5291 (1987).
  - [7] Y. Kato and A. Tanaka, J. Phys. Soc. Jpn. 63, 1277 (1994).
  - [8] S. Yamamoto, J. Phys. Soc. Jpn. 63, 4327 (1994).
  - [9] M. Hagiwara, Y. Nambu, K. Kondo, M. Kohno, H. Nakano, R. Sato, and M. Takahashi, Phys. Rev. Lett. 80, 1312 (1998).
  - [10] K. Takano, Phys. Rev. Lett. 82, 5124 (1999).
  - [11] K. Takano, Physica B 284-288, 1555 (2000).
  - [12] K. Takano, Phys. Rev. B 61, 8863 (2000).
  - [13] T. Fukui and N. Kawakami, Phys. Rev. B 56, 8799 (1997).
  - [14] I.A. A., T. Kennedy, E.H. Lieb and H. Tasaki, Phys. Rev. Lett. 59, 799 (1987).
  - [15] W. Chen and K. Hida, J. Phys. Soc. Jpn. 67, 2910 (1998).
  - [16] T. Hikihara, T. Tonegawa, M. Kaburagi, T. Nishino, S. Miyashita and H.-J. Mikeska, J. Phys. Soc. Jpn. 69, 1207 (2000).
  - [17] A special case of  $s=1$  and  $t=\frac{1}{2}$  has been partially studied; K. Takano, cond-mat/0003274 (unpublished).
  - [18] E. Lieb and D. Mattis, J. Math. Phys. 3, 749 (1962).
  - [19] The NLSM (9) stands for a general periodic spin chain, if general forms are used for  $J^{(i)}$  ( $i=0, 1, 2$ ) [10].